Determination of branches of limit points by an Asymptotic Numerical Method

Sébastien Baguet, Bruno Cochelin

European Congress on Computational Methods in Applied Sciences and Engineering
ECCOMAS 2000
Barcelona, 11-14 September 2000

DETERMINATION OF BRANCHES OF LIMIT POINTS BY AN ASYMPTOTIC NUMERICAL METHOD

S. Baguet and B. Cochelin

Laboratoire de Mécanique et d'Acoustique CNRS UPR 7051
Ecole Supérieure de Mécanique de Marseille, IMT Technopôle de Château Gombert,
13451 Marseille Cedex 20 - France
e–mail: baguet@imtumn.imt-mrs.fr

Key words: Instabilities, Fold curve, Turning points, Asymptotic Numerical Method, Extended system, Finite elements, Path following.

Abstract. *This paper deals with parameter dependence in nonlinear structural stability problems. The main purpose is the study of the influence of imperfections on a structure. This analysis implies the calculation of the so called fold curve connecting the critical points of the equilibrium path when a structural defect varies. This is traditionally achieved by adding a well-chosen constraint equation demanding the criticality of the equilibrium. The crucial feature of the paper lies in the use of the Asymptotic Numerical Method (A.N.M.) for the numerical resolution of the obtained augmented system. The theoretical framework upon which the A.N.M. is based as well as its advantages over incremental-iterative strategies are presented. The numerical isolation of an initial starting limit point is described. The extended system and its resolution with the A.N.M. are discussed. From a numerical point of view, it leads to an efficient treatment which takes the singularity of the tangent stiffness matrix into account. Emphasis is given on a geometrical shape imperfection.*

1 INTRODUCTION

We consider nonlinear systems depending on two parameters of the form

$$\boldsymbol{F}(\boldsymbol{u}, \Lambda, \lambda) = 0 \tag{1}$$

where $\boldsymbol{u} \in \mathbb{R}^n$, λ and $\Lambda \in \mathbb{R}$ and $\boldsymbol{F}$ is a continuously differentiable operator mapping from $\mathbb{R}^n \times \mathbb{R}^2$ into $\mathbb{R}^n$. Several nonlinear problems are governed by such a system, as well in chemistry as in fluid mechanics (Navier-Stokes equations) or structural mechanics (buckling, material nonlinearities, contact, ...).

This paper is more particularly concerned with sensitivity and parameter dependence for structural stability problems. This type of analysis is based on two main problems. The most common one concerns the determination of critical states and in particular the calculation of the maximal load that the structure can handle before loss of stability or snap-through. The second one is related to the study of the sensitivity of the structure to geometrical or material variations. Such imperfections can be due to manufacturing defects, unusual loadings or shocks. The question is then, how does the structure behave in presence of these imperfections ?

In the case of quasi-static linear elasticity, the governing equations of the first problem can be represented as a one-parameter system of the form

$$\boldsymbol{F}(\boldsymbol{u}, \lambda) = \boldsymbol{F}(\boldsymbol{u}) - p(\lambda) = 0 \tag{2}$$

where $\boldsymbol{F}$ stands for the internal forces, $p(\lambda)$ for the external applied loads and λ for the load parameter. The calculation of the fundamental equilibrium path of the perfect structure and the detection of the critical states along this path are commonly achieved using an incremental-iterative algorithm (Newton-like methods). The second problem implies the determination of the critical states for different values of an imperfection amplitude Λ. Indeed, when a geometric (either structural or relative to the thickness) or material imperfection is introduced within the original perfect structure, the critical state can be significantly affected. Fig. 1 shows a bifurcating point becoming a limit (or turning) point with different values of Λ. As a result, this amplitude must become an additional parameter and the system (2) becomes a two-parameter system of the form

$$\boldsymbol{F}(\boldsymbol{u}, \lambda, \Lambda) = \boldsymbol{f}(\boldsymbol{u}, \Lambda) - p(\lambda) = 0 \tag{3}$$

The main purpose of this paper is the determination of the curve $\mathcal{C}$ connecting the limit points when Λ varies. In practice, it is not judicious to calculate all the different equilibrium paths for fixed values of Λ as shown in Fig. 1. It is more advisable to proceed in two distinct steps : at first, the determination of one of the basic equilibrium paths for a given value of the additional parameter Λ and the accurate detection of a

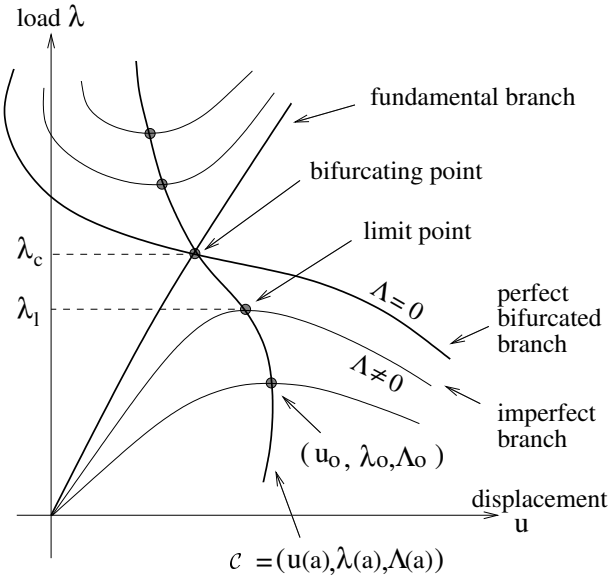

Figure 1: Perfect and imperfect equilibrium paths and limit points branch.

starting limit point on this path, and then the direct path-following of the branch $\mathcal{C}$. By this way, only the curve (called a fold curve) connecting the critical points is computed. This is accomplished by appending to the system of the nonlinear equilibrium equations $\boldsymbol{F}(\boldsymbol{u}, \lambda, \Lambda) = 0$ a constraint equation that characterizes the studied critical state. Doing so, the system (3) becomes an augmented system which reads

$$\boldsymbol{R}(\boldsymbol{u}, \boldsymbol{\varphi}, \lambda, \Lambda) = \begin{pmatrix} \boldsymbol{F}(\boldsymbol{u}, \lambda, \Lambda) \\ \boldsymbol{G}(\boldsymbol{u}, \boldsymbol{\varphi}, \Lambda) \end{pmatrix} = 0 \tag{4}$$

This method has already been addressed by Jepson and Spence [1] , Wagner and Wriggers [2], and Eriksson [3] using incremental-iterative strategies. In this paper, the imperfection analysis is reconsidered using the so called Asymptotic Numerical Method as an alternative to incremental-iterative methods. This technique which is based on high order Taylor series representations of the curves, provides crucial advantages for making the continuation of a path and detecting critical points. In Section 2, we begin with a review of the A.N.M. for tracing the fundamental path and we propose an efficient technique, also based on the A.N.M., for the detection of the critical states.

Section 3 is devoted to the determination of a fold line using the A.N.M. concept. We make a rather general presentation of the perturbation series, of the linear system to be solved and of the specific solution procedure. We close by discussing the case of a structural geometric imperfection.

2 THE BASIC EQUILIBRIUM PROBLEM AND THE A.N.M.

The aim of this Section is to set the principle of the A.N.M., to outline several interesting advantages of the method over the incremental-iterative strategies and to introduce the notations that will be used in the sequel. This method is inspired by the perturbation techniques developed by Thompson and Walker [4] and used by Noor et al. [5] for designing "reduced bases" algorithms. They have been revisited and efficiently solved by Cochelin, Damil and Potier-Ferry [6][7][8]. A continuation method has been proposed by Cochelin and is described in detail in [9].

2.1 Basic equilibrium problem

In this Section, all the parameters are supposed to be constant, excepted the load parameter. It can be seen as a particular case of the multi-parameter problem. Assuming that the external forces $p(\lambda)$ are proportional to the external load $\boldsymbol{F}_e$, the system to solve takes the form

$$\boldsymbol{F}(\boldsymbol{u},\lambda) = \boldsymbol{f}(\boldsymbol{u}) - \lambda \boldsymbol{F}_e = 0 \tag{5}$$

where $\boldsymbol{u}$ stands for the displacement and $\boldsymbol{f}$ for the internal forces vector.

2.2 A.N.M. for the calculation of the fundamental equilibrium path

2.2.1 Quadratic formulation

In the case of geometrical nonlinear elasticity, Eq. (5) is cubic with respect to $\boldsymbol{u}$. This cubic expression is not very suitable for asymptotic expansions. A quadratic expression is preferred. It is achieved by introducing the stress-strain relation as an additional equation. Eq. (5) can thus be replaced by the following equivalent system

$$\boldsymbol{F}(\boldsymbol{u},\lambda) = \left\{ \begin{array}{l} \displaystyle\int_\Omega \boldsymbol{B}^t(\boldsymbol{u})\, \boldsymbol{S}\, d\Omega - \lambda \boldsymbol{F}_e = 0 \\ \text{where } \ \boldsymbol{S} = \boldsymbol{D}\ \left(\boldsymbol{B}_l + \frac{1}{2}\boldsymbol{B}_{nl}(\boldsymbol{u})\right)\ \boldsymbol{u} \end{array} \right. \tag{6}$$

We have used the classical $\boldsymbol{B}$ operator defined by $\boldsymbol{B}(\boldsymbol{u})$=$\boldsymbol{B}_l$+$\boldsymbol{B}_{nl}(\boldsymbol{u})$ where $\boldsymbol{B}_l$ and $\boldsymbol{B}_{nl}(\boldsymbol{u})$ are the classical operators expressing the linear and nonlinear parts of the Green-Lagrange strain [10]. $\boldsymbol{S}$ is the second Piola Kirchhoff stress operator and $\boldsymbol{D}$ is the classical elasticity operator function. The first equation stands for equilibrium. It is quadratic with respect to the set of variables $(\boldsymbol{u}, \boldsymbol{S})$. The constitutive law has been introduced in order to make both equations quadratic.

2.2.2 Asymptotic expansions

Assuming that a a regular point $(\boldsymbol{u}_0, \lambda_0)$ is known, the basic idea of the A.N.M. consists in seeking the solution branch $(\boldsymbol{u}, \lambda)$ in a truncated power series form with respect to a

well chosen path parameter "a". For convenience, an expansion of the variable $\boldsymbol{S}$ is also introduced, with $\boldsymbol{S}_0 = \boldsymbol{D}\,\boldsymbol{B}(\boldsymbol{u}_0)\,\boldsymbol{u}_0$

$$\begin{aligned} \boldsymbol{u}(a) &= \boldsymbol{u}_0 + a\,\boldsymbol{u}_1 + a^2\,\boldsymbol{u}_2 + \ldots + a^n\,\boldsymbol{u}_n \\ \boldsymbol{S}(a) &= \boldsymbol{S}_0 + a\,\boldsymbol{S}_1 + a^2\,\boldsymbol{S}_2 + \ldots + a^n\,\boldsymbol{S}_n \\ \lambda(a) &= \lambda_0 + a\,\lambda_1 + a^2\,\lambda_2 + \ldots + a^n\,\lambda_n \end{aligned} \tag{7}$$

Introducing these expansions into the nonlinear problem (6) and identifying the power-like terms leads to a succession of linear problems with the form

$$\text{order 1} \quad \left\{ \begin{array}{l} \displaystyle\int_\Omega \boldsymbol{B}^t(\boldsymbol{u}_0)\,\boldsymbol{S}_1 + \boldsymbol{B}^t_{nl}(\boldsymbol{u}_1)\,\boldsymbol{S}_0\;d\Omega = \lambda_1 \boldsymbol{F}_e \\ \quad \boldsymbol{S}_1 = \boldsymbol{D}\,\boldsymbol{B}(\boldsymbol{u}_0)\,\boldsymbol{u}_1 \end{array} \right.$$

$$\text{order 2} \quad \left\{ \begin{array}{l} \displaystyle\int_\Omega \boldsymbol{B}^t(\boldsymbol{u}_0)\,\boldsymbol{S}_2 + \boldsymbol{B}^t_{nl}(\boldsymbol{u}_2)\,\boldsymbol{S}_0\;d\Omega = \lambda_2 \boldsymbol{F}_e - \int_\Omega \boldsymbol{B}^t_{nl}(\boldsymbol{u}_1)\,\boldsymbol{S}_1\;d\Omega \\ \quad \boldsymbol{S}_2 = \boldsymbol{D}\,\boldsymbol{B}(\boldsymbol{u}_0)\,\boldsymbol{u}_2 + \frac{1}{2}\,\boldsymbol{D}\,\boldsymbol{B}_{nl}(\boldsymbol{u}_1)\,\boldsymbol{u}_1 \end{array} \right.$$

$$\vdots \qquad\qquad \vdots$$

$$\text{order } p \quad \left\{ \begin{array}{l} \displaystyle\int_\Omega \boldsymbol{B}^t(\boldsymbol{u}_0)\,\boldsymbol{S}_p + \boldsymbol{B}^t_{nl}(\boldsymbol{u}_p)\,\boldsymbol{S}_0\;d\Omega = \lambda_p \boldsymbol{F}_e - \int_\Omega \sum_{r=1}^{p-1} \boldsymbol{B}^t_{nl}(\boldsymbol{u}_r)\,\boldsymbol{S}_{p-r}\;d\Omega \\ \quad \boldsymbol{S}_p = \boldsymbol{D}\,\boldsymbol{B}(\boldsymbol{u}_0)\,\boldsymbol{u}_p + \frac{1}{2}\,\boldsymbol{D}\sum_{r=1}^{p-1} \boldsymbol{B}_{nl}(\boldsymbol{u}_r)\,\boldsymbol{u}_{p-r} \end{array} \right. \tag{8}$$

Introducing the notation

$$\boldsymbol{S}_p^{nl} = \frac{1}{2}\,\boldsymbol{D}\sum_{r=1}^{p-1} \boldsymbol{B}_{nl}(\boldsymbol{u}_r)\,\boldsymbol{u}_{p-r} \tag{9}$$

the second equation of (8) can be rewritten as

$$\boldsymbol{S}_p = \boldsymbol{D}\,\boldsymbol{B}(\boldsymbol{u}_0)\,\boldsymbol{u}_p + \boldsymbol{S}_p^{nl} \tag{10}$$

The problem (8) at order p is a classical linearized elasticity problem where $\boldsymbol{S}_p^{nl}$ stands for a pre-stress term and $\int_\Omega \sum \boldsymbol{B}^t_{nl}(\boldsymbol{u}_r)\,\boldsymbol{S}_{p-r} d\Omega$ for a prescribed load. There is still one unknown (λ_p) at this stage. It will disappear with the choice of the path parameter "a". Here we take

$$a = \frac{1}{s^2}\;\left[\;(\boldsymbol{u}-\boldsymbol{u}_0)^t\,.\,\boldsymbol{u}_1 + (\lambda-\lambda_0)\,\lambda_1\;\right] \tag{11}$$

This choice which is inspired by the arc-length continuation method identifies a as the projection of the increments $\boldsymbol{u}-\boldsymbol{u}_0$ and $\lambda-\lambda_0$ on the tangent direction. At order 1 Eq. (7) and (11) leads to

$$\boldsymbol{u}_1^t\,.\,\boldsymbol{u}_1 + \lambda_1\,\lambda_1 = s^2 \tag{12}$$

where s is a given value that fixes the length of the tangent vector. It must be noticed that it does not set the step length. This one is based on a residual criterium that will be discussed in Section 2.2.4. At order p, the relation reads

$$\boldsymbol{u}_1^t \,.\, \boldsymbol{u}_p + \lambda_1 \, \lambda_p = 0 \tag{13}$$

The system (8) and (13) uniquely determine $\boldsymbol{u}_p$, $\boldsymbol{S}_p$, λ_p.

2.2.3 Finite element method

The previous linear systems can be efficiently solved by a F.E.M. Each of these systems contains an equilibrium equation in $\boldsymbol{u}$ and $\boldsymbol{S}$ and a constitutive equation. Since classical FEM are based on a displacement formulation, it is necessary to transform the first equation into a pure displacement problem. This can be easily done by replacing the expression of $\boldsymbol{S}$ in the equilibrium. Thus, each linear problem (8) is transformed into into a pure displacement problem in $\boldsymbol{u}_p$ and a stress-strain relation which gives the stress $\boldsymbol{S}_p$. After discretization, the displacement problem at order p ($p \geq 2$) reads

$$\begin{aligned} &\boldsymbol{K}_t \, \boldsymbol{u}_p = \lambda_p \, \boldsymbol{F}_e + \boldsymbol{F}_p^{nl} \\ &\boldsymbol{u}_1^t \, \boldsymbol{u}_p + \lambda_1 \, \lambda_p = 0 \end{aligned} \tag{14}$$

where $\boldsymbol{K}_t = \boldsymbol{K}_t(\boldsymbol{u}_0, \boldsymbol{S}_0)$ is the classical tangent stiffness matrix at the starting point $(\boldsymbol{u}_0, \lambda_0)$. $\boldsymbol{F}_e$ is the vector of external loads and $\boldsymbol{F}_p^{nl}$ is a load vector which depends only on the previous orders and reads

$$\boldsymbol{F}_p^{nl} = -\int_\Omega \boldsymbol{B}(\boldsymbol{u}_0) \, \boldsymbol{S}_p^{nl} - \sum_{r=1}^{p-1} \boldsymbol{B}_{nl}^t(\boldsymbol{u}_r) \, \boldsymbol{S}_{p-r} \, d\Omega \tag{15}$$

At this stage, many remarks can be made :
- All the linear systems have the same $\boldsymbol{K}_t$ matrix, hence only one matrix decomposition is required to compute the terms of the series. It allows to compute the series up to high orders (20 or 30 in practice) since the extra calculation cost consists only in the assembly of the supplementary $\boldsymbol{F}_p^{nl}$ vectors and in a back-substitution for each order.
- The problem at order 1 gives the tangent direction $(\boldsymbol{u}_1, \lambda_1)$. It corresponds to the predictor step in the incremental-iterative Newton-Raphson algorithm. The next problems can then be solved recursively since they are simple linearized elasticity problems depending on the previous orders. This algorithm is thus very easy to implement.
- The series (7) generally allows to compute a large part of the solution branch that starts at $(\boldsymbol{u}_0, \lambda_0)$ [7].

2.2.4 The continuation method

Because of the limited radius of convergence of the series, this process must be applied several times, quite in the same way as the classical continuation methods. The length

of each step can be determined by a residual criterium (see Cochelin [9]). For series truncated at order N, the maximal value of a for which the solution satisfies a requested precision ε is given by

$$a_M = \left(\frac{\varepsilon}{\|\boldsymbol{F}_{N+1}^{nl}\|} \right)^{\frac{1}{N+1}} \tag{16}$$

By applying the method from a successively updated new starting point, we can determine a complex solution branch in a step by step manner. This procedure is very robust and completely automatic from the user's point of view. Moreover, the step length is always optimal.

To illustrate the capabilities of this method , an example is provided in Fig. 2. It is a classical buckling case which involves limit points and snap-through phenomenon. The geometrical and material properties of the cylindrical panel are given in Fig. 2. For symmetry reasons, only a quarter of the panel was discretized, using a mesh with 200 triangular DKT shell elements [11] and 726 degrees of freedom. With series truncated at order 30 and an accuracy $\varepsilon = 10^{-6}$ monitored by Eq. (16), the interesting part of the curve is fully described with only four steps.

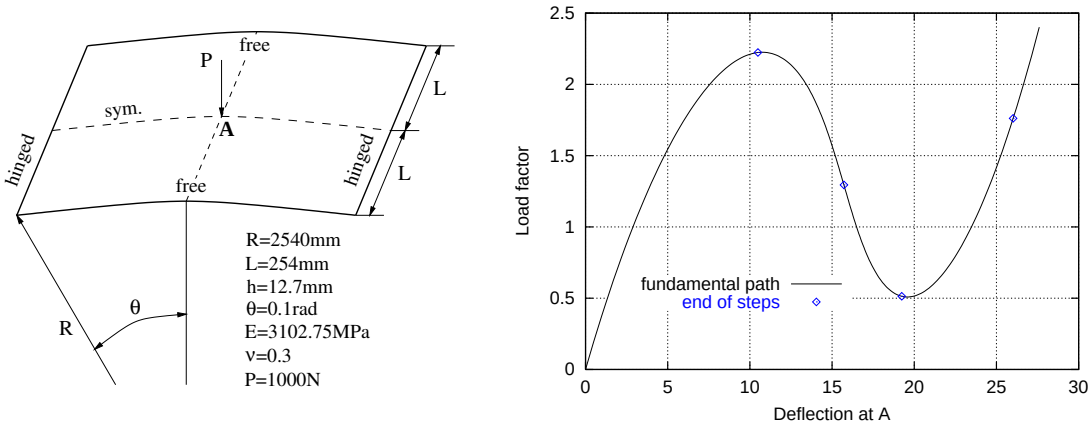

Figure 2: Cylindrical panel : problem definition and load-deflection curves for the basic equilibrium problem with series truncated at order 30 and $\varepsilon = 10^{-6}$.

2.3 Detection of critical states on the equilibrium path

Before following the fold curve, a starting limit point must be precisely detected on the fundamental path. The method presented here consists in detecting the critical states by the mean of a perturbed equilibrium problem that will be subsequently solved with the A.N.M. It has been first introduced by Boutyour [16] and used by Vannucci et al. [17].

The singular point is searched on the equilibrium path defined by (3) for given values Λ_0 of the additional parameters which define the initial imperfection. The resulting governing

equation

$$\boldsymbol{F}(\boldsymbol{u}, \Lambda_0, \lambda) = \boldsymbol{f}(\boldsymbol{u}, \Lambda_0) - p(\lambda) = 0 \tag{17}$$

can be seen as a particular case of the basic equilibrium problem (5). Thus, the procedure given in Section 2 can be applied for the calculation of the equilibrium path.

The detection of the criticality is made through the introduction of a perturbation into the system. This perturbed problem is described by

$$\boldsymbol{f}_{,\boldsymbol{u}} \,.\, \boldsymbol{\Delta u} = \Delta\mu \, \boldsymbol{f}_e \tag{18}$$

where $\boldsymbol{\Delta u}$ is the displacement response of the structure to the load perturbation $\Delta\mu \, \boldsymbol{f}_e$. For a fixed displacement perturbation $\boldsymbol{\Delta u}$, it is the point where the load response $\Delta\mu$ tends to zero. When $\boldsymbol{\Delta u}$ is fixed, $\Delta\mu$ can be seen as a stiffness measurement. Hence, the singular points correspond to the null values of the bifurcation indicator $\Delta\mu$. The system (18) consists of n equations and involves $n+1$ unknowns, the n components of $\boldsymbol{\Delta u}$ and $\Delta\mu$. An additional condition must be provided for (18) to admit a unique solution for each regular point of the fundamental path. Since we have decided to fix the displacement perturbation rather than the load perturbation, this condition will be chosen such as

$$\|\boldsymbol{\Delta u}\| = 1 \tag{19}$$

Equations (18) and (19) form a well-posed system which will be solved using the A.N.M.

The critical points correspond to the values a_c of the parameter a for which $\Delta\mu(a)$ is zero, and the corresponding critical load is obtained by $\lambda(a_c)$. It must be noticed that this procedure does not only provide the critical load. The associated eigenvector is also given by $\boldsymbol{\Delta u}(a_c)$. As a result, all the initial information that is required for the calculation of the fold curve of Section 3 is supplied by this procedure. Moreover, the numerical precision of this information can be monitored through the use of a residual criterium in order to satisfy a given precision ε. A very accurate starting point for the fold curve can thus be obtained.

The example presented in Fig. 3 demonstrates the capabilities of this algorithm to detect singular points as well as limit points. The geometry of the panel is the same as in Fig. 2, excepted for the thickness which is now $h = 6.35mm$. This value leads to a far more complicated equilibrium path. One half of the panel was discretized in order to get the bifurcated path. For symmetry reasons, it does not appear if only one quarter is considered. Series were truncated at order 30. Two limit points and two bifurcation points, connected by a bifurcated path, were detected. Both singular points and their associated eigenmodes were obtained with a required accuracy $\varepsilon = 10^{-8}$. Any of the limit point can then be used as a starting point for the computation of the fold curve, as described in Section 3.

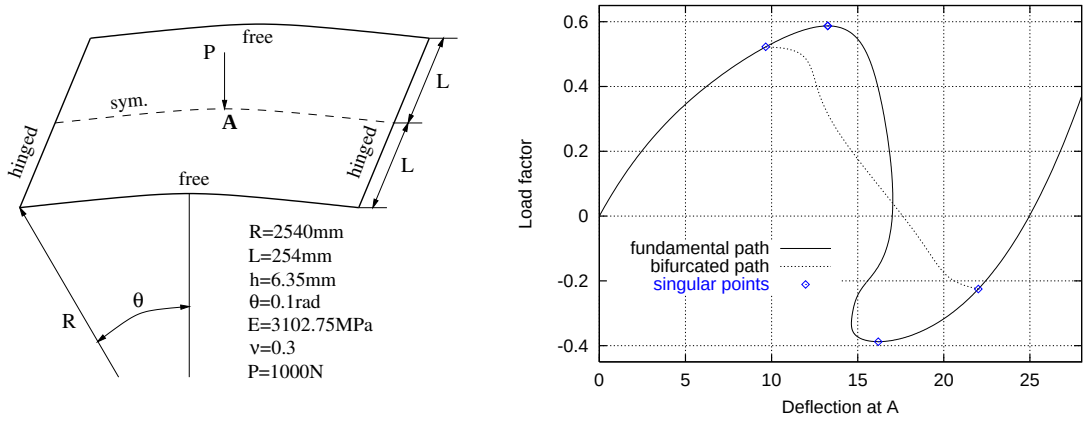

Figure 3: Cylindrical panel : problem definition and detected singular points on the fundamental path of the basic equilibrium problem

3 DIRECT COMPUTATION OF CRITICAL PATHS

We now consider the multi-parameter nonlinear system

$$\boldsymbol{F}(\boldsymbol{u}, \lambda, \Lambda) = \boldsymbol{f}(\boldsymbol{u}, \Lambda) - p(\lambda) = 0 \tag{20}$$

We intend to compute the fold curve connecting the singular points of $\boldsymbol{F}$. To do so, additional information characterizing these singular points must be provided, yielding a so called extended or augmented system.

3.1 The augmented problem

Many alternatives have been proposed in the literature to define the criticality, the simplest of them lying on the study of the determinant of the tangent stiffness matrix. However, this criterium is not well suited for a numerical study. The method presented here has been first introduced by Keener and Keller [12], subsequently used by Moore and Spence [13], Jepson and Spence [1], and numerically investigated by Wriggers and Simo [14] and Eriksson et. al [15] among others. It is based on the appearance of a null eigenvalue for the tangent operator $\boldsymbol{K}_T = \boldsymbol{F}_{,\boldsymbol{u}}$ at simple critical states. The corresponding extended system reads

$$\boldsymbol{R}\left(\boldsymbol{u}, \boldsymbol{\varphi}, \Lambda, \lambda\right) = \begin{pmatrix} \boldsymbol{F}\left(\boldsymbol{u}, \Lambda, \lambda\right) \\ \boldsymbol{F}_{,\boldsymbol{u}}\left(\boldsymbol{u}, \Lambda, \lambda\right) \cdot \boldsymbol{\varphi} \\ \|\boldsymbol{\varphi}\| - 1 \end{pmatrix} = 0 \tag{21}$$

where $\boldsymbol{\varphi}$ is the eigenvector associated with the null eigenvalue. The last normalization condition ensures its uniqueness.

For a fixed value $\Lambda = \Lambda_0$ of the additional parameters, this augmented problem gives a singular point of $\boldsymbol{F}$, either a bifurcating point or a turning point with respect to λ.

When Λ varies, it provides the entire fold curve connecting the singular points of $\boldsymbol{F}$, both bifurcating or turning points with respect to λ and Λ.

3.2 Asymptotic Numerical Method

In this Section we solve the previous extended system (21) using the Asymptotic Numerical Method introduced in Section 2.2.

As previously stated, it is more convenient to turn the basic equations into a quadratic formulation in order to apply the asymptotic expansions. This stage is probably the most complex one of the procedure. The difficulty lies on the number of additional variables which need to be introduced to reduce the degree of the equations with respect to the different unknowns $\boldsymbol{u}$, $\boldsymbol{\varphi}$, λ and Λ. This procedure will be detailed in Section 3.4 in the case of a geometrical shape imperfection. Here, we do not enter into these details. We assume that the fold line can be represented by a power series of the form

$$\begin{aligned}
\boldsymbol{u}(a) &= \boldsymbol{u}_0 + a\,\boldsymbol{u}_1 + a^2\,\boldsymbol{u}_2 + \ldots + a^n\,\boldsymbol{u}_n \\
\boldsymbol{\varphi}(a) &= \boldsymbol{\varphi}_0 + a\,\boldsymbol{\varphi}_1 + a^2\,\boldsymbol{\varphi}_2 + \ldots + a^n\,\boldsymbol{\varphi}_n \\
\lambda(a) &= \lambda_0 + a\,\lambda_1 + a^2\,\lambda_2 + \ldots + a^n\,\lambda_n \\
\Lambda(a) &= \Lambda_0 + a\,\Lambda_1 + a^2\,\Lambda_2 + \ldots + a^n\,\Lambda_n
\end{aligned} \tag{22}$$

where $(\boldsymbol{u}_0, \boldsymbol{\varphi}_0, \Lambda_0, \lambda_0)$ is supposed to be a regular initial solution point of $\boldsymbol{R}$. Replacing (22) into the nonlinear problem (21) and applying the technique described in Section 2.2 leads to the final discretized linear problem at order p

$$\begin{bmatrix} \boldsymbol{K}_T & 0 & \boldsymbol{F}_1 & -\boldsymbol{F}_e \\ \boldsymbol{K}_{\boldsymbol{\varphi}} & \boldsymbol{K}_T & \boldsymbol{F}_2 & 0 \\ 0 & \boldsymbol{\varphi}_0^t & 0 & 0 \\ \boldsymbol{u}_1^t & 0 & \Lambda_1 & \lambda_1 \end{bmatrix} \begin{bmatrix} \boldsymbol{u}_p \\ \boldsymbol{\varphi}_p \\ \Lambda_p \\ \lambda_p \end{bmatrix} = \begin{bmatrix} \boldsymbol{F}_p^{nl} \\ \boldsymbol{G}_p^{nl} \\ h_p^{nl} \\ 0 \end{bmatrix} \quad \begin{matrix} \text{size n} \\ \text{size n} \\ \text{size 1} \\ \text{size 1} \end{matrix} \tag{23}$$

The two vectors $\boldsymbol{F}_1$, $\boldsymbol{F}_2$ and the matrix $\boldsymbol{K}_{\boldsymbol{\varphi}}$ are introduced to shorten the notations. $\boldsymbol{F}_1$ and $\boldsymbol{F}_2$ stand for $f_{,\Lambda}$ and $f_{,\boldsymbol{u}\Lambda} \cdot \boldsymbol{\varphi}_0$ and $\boldsymbol{K}_{\boldsymbol{\varphi}}$ is the matrix $f_{,\boldsymbol{u}\boldsymbol{u}} \cdot \boldsymbol{\varphi}_0 = \boldsymbol{K}_{T,\boldsymbol{u}} \cdot \boldsymbol{\varphi}$. The r.h.s. vectors $\boldsymbol{F}_p^{nl}$ and $\boldsymbol{G}_p^{nl}$ and the scalar h_p^{nl} result of summations of quadratic products depending only on the solutions at previous orders. The nl subscript is used to easily distinguish this r.h.s from the other terms. The matrix $\boldsymbol{K}_{\boldsymbol{\varphi}}$ is the same whatever the imperfection. The expression of the vectors $\boldsymbol{F}_1$ and $\boldsymbol{F}_2$ and the r.h.s. depends on the type of imperfection introduced within the structure. Their expressions will be detailed in Section 3.4. The last equation of the system (23) is an extended version of Eq. (13).

3.3 Procedure to solve the augmented matrix system

At order 1, the terms $\boldsymbol{F}_p^{nl}$, $\boldsymbol{G}_p^{nl}$ and h_p^{nl} are null and the system (23) takes the particular form

$$\left[\begin{array}{cccc} \boldsymbol{K}_T & 0 & \boldsymbol{F}_1 & -\boldsymbol{F}_e \\ \boldsymbol{K}_{\boldsymbol{\varphi}} & \boldsymbol{K}_T & \boldsymbol{F}_2 & 0 \\ 0 & \boldsymbol{\varphi}_0^t & 0 & 0 \\ \boldsymbol{u}_1^t & 0 & \Lambda_1 & \lambda_1 \end{array}\right] \left[\begin{array}{c} \boldsymbol{u}_1 \\ \boldsymbol{\varphi}_1 \\ \Lambda_1 \\ \lambda_1 \end{array}\right] = \left[\begin{array}{c} 0 \\ 0 \\ 0 \\ s^2 \end{array}\right] \tag{24}$$

In practice, the direct resolution of the complete system (24) is avoided. A gauss-like elimination is used in order to consider only subsystems of size n involving the $\boldsymbol{K}_T$ matrix. Such a block-elimination scheme can be found in Wriggers and Simo [14]. Its main interest relies on the fact that only the classical $\boldsymbol{K}_T$ matrix needs to be decomposed, thus saving a large amount of calculation time.

Besides this particular procedure, another numerical difficulty must be pointed out. Since all the solution points of $\boldsymbol{R}$ are singular ones of $\boldsymbol{F}$, the $\boldsymbol{K}_T$ matrix is singular all along the fold line connecting the computed solution points. That means that the classical matrix decomposition techniques cannot be used. A special procedure, based on Lagrange multipliers, is introduced to bypass this problem [8]. The solution vectors are decomposed into their projection on $\boldsymbol{\varphi}_0$ and orthogonal parts

$$\begin{array}{rcll} \boldsymbol{u}_1 & = & \alpha_1 \boldsymbol{\varphi}_0 + \lambda_1 \boldsymbol{v}_1^{\perp} + \eta_1 \boldsymbol{v}_2^{\perp} , & \alpha_1 \in \mathbb{R} \\ \boldsymbol{\varphi}_1 & = & \alpha_2 \boldsymbol{\varphi}_0 + \lambda_1 \boldsymbol{p}_1^{\perp} + \eta_1 \boldsymbol{p}_2^{\perp} , & \alpha_2 \in \mathbb{R} \end{array} \tag{25}$$

with the conditions

$$\begin{array}{ll} \boldsymbol{\varphi}_0^t \boldsymbol{v}_1^{\perp} = 0 & \boldsymbol{\varphi}_0^t \boldsymbol{v}_2^{\perp} = 0 \\ \boldsymbol{\varphi}_0^t \boldsymbol{p}_1^{\perp} = 0 & \boldsymbol{\varphi}_0^t \boldsymbol{p}_2^{\perp} = 0 \end{array} \tag{26}$$

These orthogonality conditions are enforced through the use of a Lagrange multiplier μ and the orthogonal parts of $\boldsymbol{u}_1$ and $\boldsymbol{\varphi}_1$ are obtained by systems such as

$$\left[\begin{array}{cc} \boldsymbol{K}_T & \boldsymbol{\varphi}_0 \\ \boldsymbol{\varphi}_0^t & 0 \end{array}\right] \left[\begin{array}{c} \boldsymbol{v}_1^{\perp} \\ \mu \end{array}\right] = \left[\begin{array}{c} \boldsymbol{F}_e \\ 0 \end{array}\right] \tag{27}$$

Premultiplying the two first equations of (24) by $\boldsymbol{\varphi}_0^t$ yields two compatibility relation between Λ_1 and λ_1

$$\Lambda_1 \boldsymbol{\varphi}_0^t \boldsymbol{F}_1 - \lambda_1 \boldsymbol{\varphi}_0^t \boldsymbol{F}_e = 0 \tag{28}$$

$$\alpha_1 \boldsymbol{\varphi}_0^t \boldsymbol{K}_{\boldsymbol{\varphi}} \boldsymbol{\varphi}_0 + \lambda_1 \boldsymbol{\varphi}_0^t \boldsymbol{K}_{\boldsymbol{\varphi}} \boldsymbol{v}_1^{\perp} + \eta_1 \left(\boldsymbol{\varphi}_0^t \boldsymbol{K}_{\boldsymbol{\varphi}} \boldsymbol{v}_2^{\perp} + \boldsymbol{F}_2 \right) = 0 \tag{29}$$

These two scalar equations and the two last equations of (24) lead to a 4 by 4 linear system which provides α_1, α_2, λ_1 and η_1. The final solution at order 1 can then be obtained

by (25).

The resolution is slightly different at order p than before because of the r.h.s. terms of the system (23). Nevertheless, the block-elimination procedure remains the same. That is why the resolution will not be detailed here. Despite the additional r.h.s. terms, the global calculation cost remains the same. Indeed, the solutions can be expressed as the sum of a term which is proportional to the solutions at order 1 and a term which come from the new r.h.s. vectors. As a result, only two back-substitutions are needed to compute all the terms at order p.

3.4 Geometrical shape imperfection

In section 2.2.1, emphasis has been put on the fact that the transformation of the governing equations into a quadratic form was crucial for the asymptotic expansions. The main purpose of this section is to provide a general procedure for the obtaining of such a formulation. This procedure is based on the introduction of well chosen extra variables, thus augmenting the number of equations to be solved but reducing the degree of each of the governing equations. This required procedure does not restrict the range of problems which can be treated by the A.N.M. The expression of the vectors $\boldsymbol{F}_1$, $\boldsymbol{F}_2$, $\boldsymbol{F}_p^{nl}$ and $\boldsymbol{G}_p^{nl}$ of the discretized augmented system (23) will be detailed here for a geometrical shape imperfection.

A schematic structure with a shape imperfection $\boldsymbol{u}^\star$ is presented in Fig. 4.

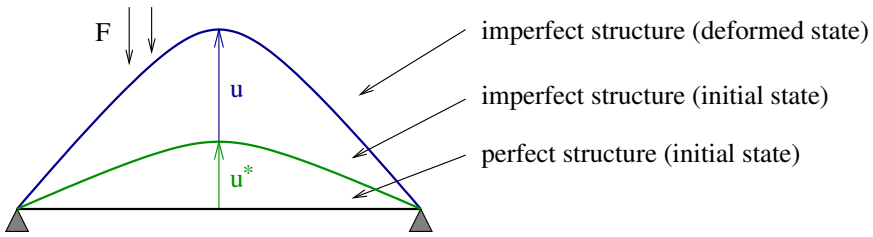

Figure 4: Structure with a geometrical shape imperfection

The strain $\boldsymbol{\gamma}$ of the deformed imperfect structure is deduced from

$$\boldsymbol{\gamma}(\boldsymbol{u}, \boldsymbol{u}^\star) = \boldsymbol{\gamma}(\boldsymbol{u} + \boldsymbol{u}^\star) - \boldsymbol{\gamma}(\boldsymbol{u}^\star) \tag{30}$$

where $\boldsymbol{\gamma}$ is the classical Green Lagrange strain defined as

$$\boldsymbol{\gamma}(\boldsymbol{u}) = \frac{1}{2}(\nabla \boldsymbol{u} + \nabla^t \boldsymbol{u}) + \frac{1}{2}(\nabla \boldsymbol{u}\, \nabla^t \boldsymbol{u}) = \boldsymbol{\gamma}^l(\boldsymbol{u}) + \boldsymbol{\gamma}^{nl}(\boldsymbol{u}, \boldsymbol{u}) \tag{31}$$

Combined with (31), (30) becomes

$$\boldsymbol{\gamma}(\boldsymbol{u}, \boldsymbol{u}^\star) = \boldsymbol{\gamma}^l(\boldsymbol{u}) + \boldsymbol{\gamma}^{nl}(\boldsymbol{u}, \boldsymbol{u}) + 2\,\boldsymbol{\gamma}^{nl}(\boldsymbol{u}, \boldsymbol{u}^\star) \tag{32}$$

Compared to the classical expression (31) of the strain, there is a new term $\boldsymbol{\gamma}^{nl}(\boldsymbol{u},\boldsymbol{u}^\star)$ which is bilinear with respect to $\boldsymbol{u}$ and $\boldsymbol{u}^\star$. In order to get a scalar extra parameter, the imperfection is written as

$$\boldsymbol{u}^\star = \eta\,\boldsymbol{u}_0^\star \tag{33}$$

where $\boldsymbol{u}_0^\star$ is a fixed displacement which gives the shape of the imperfection and η is its amplitude. Using the notations introduced in Section 2, the governing equations of the imperfect structure can then be expressed as

$$\boldsymbol{F}(\boldsymbol{u},\eta,\lambda) = \left\{ \begin{array}{l} \displaystyle\int_\Omega \boldsymbol{B}^t(\boldsymbol{u})\,\boldsymbol{S} + \eta\,\boldsymbol{B}_{nl}^t(\boldsymbol{u}_0^\star)\,\boldsymbol{S}\;d\Omega - \lambda\boldsymbol{F}_e = 0 \\ \quad \boldsymbol{S} = \boldsymbol{D}\;\left(\boldsymbol{B}_l + \frac{1}{2}\boldsymbol{B}_{nl}(\boldsymbol{u}) + \eta\,\boldsymbol{B}_{nl}(\boldsymbol{u}_0^\star)\right)\boldsymbol{u} \end{array} \right. \tag{34}$$

and the constraint equation reads

$$\boldsymbol{F}_{,\boldsymbol{u}}\,(\boldsymbol{u},\eta,\lambda)\cdot\boldsymbol{\varphi} = \left\{ \begin{array}{l} \displaystyle\int_\Omega \boldsymbol{B}^t(\boldsymbol{u})\,\boldsymbol{\Psi} + \eta\,\boldsymbol{B}_{nl}^t(\boldsymbol{u}_0^\star)\,\boldsymbol{\Psi} + \boldsymbol{B}_{nl}^t(\boldsymbol{\varphi})\,\boldsymbol{S}\;d\Omega = 0 \\ \quad \boldsymbol{\Psi} = \boldsymbol{D}\;\left(\boldsymbol{B}_l + \boldsymbol{B}_{nl}(\boldsymbol{u}) + \eta\,\boldsymbol{B}_{nl}(\boldsymbol{u}_0^\star)\right)\boldsymbol{\varphi} \end{array} \right. \tag{35}$$

where $\boldsymbol{\Psi}$ is the stress associated with the null eigenvector $\boldsymbol{\varphi}$. Eq. (34) is quadratic with respect to the variable set $(\boldsymbol{u},\boldsymbol{S},\eta,\lambda)$ and (35) is quadratic with respect to $(\boldsymbol{u},\boldsymbol{S},\boldsymbol{\varphi},\boldsymbol{\Psi},\eta,\lambda)$.

The next step consists in developing each of the variables in a power series form. Introducing the mixed variable $\boldsymbol{U} = \{\boldsymbol{u},\boldsymbol{S},\boldsymbol{\varphi},\boldsymbol{\Psi},\eta,\lambda\}^t$, the series expansion reads

$$\boldsymbol{U}(a) = \boldsymbol{U}_0 + a\,\boldsymbol{U}_1 + a^2\,\boldsymbol{U}_2 + \ldots + a^n\,\boldsymbol{U}_n \tag{36}$$

where $(\boldsymbol{u}_0,\boldsymbol{S}_0,\boldsymbol{\varphi}_0,\boldsymbol{\Psi}_0,\eta_0,\lambda_0)$ is supposed to be a regular initial solution point. The introduction of the series into (34) and (35) leads at order p ($p\geq 2$) to

$$\left\{ \begin{array}{l} \displaystyle\int_\Omega \tilde{\boldsymbol{B}}_0^t\,\boldsymbol{S}_p + \boldsymbol{B}_{nl}^t(\boldsymbol{u}_p)\,\boldsymbol{S}_0 + \eta_p\,\boldsymbol{B}_{nl}^t(\boldsymbol{u}_0^\star)\,\boldsymbol{S}_0\;d\Omega = \lambda_p\boldsymbol{F}_e - \int_\Omega \sum_{r=1}^{p-1} \boldsymbol{B}_{nl}^t(\boldsymbol{u}_r + \eta_r\,\boldsymbol{u}_0^\star)\,\boldsymbol{S}_{p-r}\;d\Omega \\ \quad \boldsymbol{S}_p = \boldsymbol{D}\;\left(\tilde{\boldsymbol{B}}_0\,\boldsymbol{u}_p + \eta_p\,\boldsymbol{B}_{nl}(\boldsymbol{u}_0)\,\boldsymbol{u}_0^\star\right) + \boldsymbol{S}_p^{nl} \\ \displaystyle\int_\Omega \tilde{\boldsymbol{B}}_0^t\,\boldsymbol{\Psi}_p + \boldsymbol{B}_{nl}^t(\boldsymbol{\varphi}_p)\,\boldsymbol{S}_0 + \boldsymbol{B}_{nl}^t(\boldsymbol{u}_p)\,\boldsymbol{\Psi}_0 + \eta_p\,\boldsymbol{B}_{nl}^t(\boldsymbol{u}_0^\star)\,\boldsymbol{\Psi}_0 + \eta_p\,\boldsymbol{B}_{nl}^t(\boldsymbol{\varphi}_0)\,\boldsymbol{S}_p\;d\Omega \\ \qquad\qquad = -\displaystyle\int_\Omega \sum_{r=1}^{p-1} \boldsymbol{B}_{nl}^t(\boldsymbol{\varphi}_r)\,\boldsymbol{S}_{p-r}\;d\Omega - \int_\Omega \sum_{r=1}^{p-1} \boldsymbol{B}_{nl}^t(\boldsymbol{u}_r + \eta_r\,\boldsymbol{u}_0^\star)\,\boldsymbol{\Psi}_{p-r}\;d\Omega \\ \quad \boldsymbol{\Psi}_p = \boldsymbol{D}\;\left(\tilde{\boldsymbol{B}}_0\,\boldsymbol{\varphi}_p + \boldsymbol{B}_{nl}(\boldsymbol{\varphi}_0)\,(\boldsymbol{u}_p + \eta_p\,\boldsymbol{u}_0^\star)\right) + \boldsymbol{\Psi}_p^{nl} \end{array} \right. \tag{37}$$

$\tilde{\boldsymbol{B}}_0$ has been introduced to shorten the notations and stands for $\boldsymbol{B}(\boldsymbol{u}_0 + \eta_0\,\boldsymbol{u}_0^\star)$. Because of the introduction of the imperfection, the expressions of $\boldsymbol{S}_p^{nl}$ and $\boldsymbol{\Psi}_p^{nl}$ are slightly more

complicated than in Section 2.2. They will not been detailed here. In order to perform an F.E.M., $\boldsymbol{S}_p$ and $\boldsymbol{\Psi}_p$ are replaced in the the equilibrium and the constraint equations. After discretization, it yields the two following displacement problems

$$\begin{aligned} &\boldsymbol{K}_t\,\boldsymbol{u}_p + \eta_p\,\boldsymbol{F}_1 = \lambda_p\,\boldsymbol{F} + \boldsymbol{F}_p^{nl} \\ &\boldsymbol{K}_{\boldsymbol{\varphi}}\,\boldsymbol{u}_p + \boldsymbol{K}_T\,\boldsymbol{\varphi}_p + \eta_p\,\boldsymbol{F}_2 = \boldsymbol{G}_p^{nl} \end{aligned} \tag{38}$$

where $\boldsymbol{K}_t = \boldsymbol{K}_t\left(\boldsymbol{u}_0 + \eta_0\boldsymbol{u}_0^\star, \boldsymbol{S}_0\right)$ is the tangent stiffness matrix at the starting point $(\boldsymbol{u}_0, \eta_0, \lambda_0)$. The vectors $\boldsymbol{F}_p^{nl}$ and $\boldsymbol{G}_p^{nl}$ depend only on the previous orders. They can easily be inferred from (37). The expressions of the two vectors $\boldsymbol{F}_1$ and $\boldsymbol{F}_2$ depend on the type of imperfection. In the present case, they read

$$\begin{aligned} \boldsymbol{F}_1 &= \int_\Omega \left(\tilde{\boldsymbol{B}}_0^t\,\boldsymbol{D}\,\boldsymbol{B}_{nl}(\boldsymbol{u}_0) + \boldsymbol{G}^t\,\hat{\boldsymbol{S}}_0\,\boldsymbol{G}\right)\,\boldsymbol{u}_0^\star\,d\Omega \\ \boldsymbol{F}_2 &= \int_\Omega \left(\tilde{\boldsymbol{B}}_0^t\,\boldsymbol{D}\,\boldsymbol{B}_{nl}(\boldsymbol{\varphi}_0) + \boldsymbol{B}_{nl}(\boldsymbol{\varphi}_0)\,\boldsymbol{D}\,\boldsymbol{B}_{nl}(\boldsymbol{u}_0) + \boldsymbol{G}^t\,\hat{\boldsymbol{\Psi}}_0\,\boldsymbol{G}\right)\,\boldsymbol{u}_0^\star\,d\Omega \end{aligned} \tag{39}$$

The matrices $\hat{\boldsymbol{S}}_0$ and $\hat{\boldsymbol{\Psi}}_0$ contain components of the stress vectors $\boldsymbol{S}_0$ and $\boldsymbol{\Psi}_0$, and $\boldsymbol{G}$ is the gradient matrix of the shape functions.

Two additional equations are yet missing. The first one is the normalization condition on $\boldsymbol{\varphi}$. It is exactly the same than in the general case. The second one fixes the path parameter "a" of the fold line. It is chosen such as

$$\boldsymbol{u}_1^t\,\boldsymbol{u}_p + \eta_1\,\eta_p + \lambda_1\,\lambda_p = 0 \tag{40}$$

Putting together these two additional equations and the system (38) yields an augmented system with the same form as (23). The procedure introduced in Section 3.3 can then be used to solve it.

4 CONCLUSIONS

The paper has discussed parameter dependent problems for structural instability. A procedure for the direct calculation of paths connecting limit points when an extra parameter varies has been presented. The crucial feature of the paper lies in the use of the Asymptotic Numerical Method (A.N.M.) for each step of the computation of these so called fold curves : the description of the fundamental path, the precise detection of an starting limit point and the path following on the fold curve. The resulting continuation algorithm is thus completely automatic from the user's point of view and very robust.

We have detailed the procedure in the case a geometric shape imperfection. It should not be seen as a restrictive example, but rather as a general method. We plan to apply it to a thickness imperfection in order to simulate corrosion.

In this paper, we have focused on the theoretical aspects of the method. The numerical implementation is still in progress. Relevant examples will be presented during the colloquium. Reference examples for numerical comparison can be found in Eriksson [15].

REFERENCES

[1] A. Jepson and A. Spence. Folds in solutions of two parameter systems and their calculation. Part I. *SIAM J. Numer. Anal.*, **22**, (1985) 347–368.

[2] W. Wagner and P. Wriggers. Calculation of bifurcation points via fold curves. In W. Wagner and P. Wriggers (eds.), *Nonlinear Computational Mechanics*, 69–84. Springer-Verlag, Berlin Heidelberg (1991).

[3] A. Eriksson. Equilibrium subsets for multi-parametric structural analysis. *Comput. Methods Appl. Mech. Engrg.*, **140**, (1997) 305–327.

[4] J. Thompson and A. Walker. The nonlinear perturbation analysis of discrete structural systems. *Int. J. Solids Structures*, **4**, (1968) 757–758.

[5] A. Noor and J. Peters. Reduced basis technique for nonlinear analysis of structures. *AIAA Journal - N4*, **18**, (1980) 455–462.

[6] N. Damil and M. Potier-Ferry. A new method to compute perturbed bifurcations: application to the buckling of imperfect elastic structures. *International Journal of Engineering Sciences - N9*, **28**, (1990) 943–957.

[7] B. Cochelin, N. Damil and M. Potier-Ferry. The Asymptotic-Numerical-Method: an efficient perturbation technique for nonlinear structural mechanics. *Revue Européenne des Eléments Finis*, **3**, (1994) 281–297.

[8] L. Azrar, B. Cochelin, N. Damil and M. Potier-Ferry. An asymptotic numerical method to compute the post-buckling behavior of elastic plates and shells. *Int. J. Numer. Meth. Eng.*, **36**, (1993) 1251–1277.

[9] B. Cochelin. A path following technique via an asymptotic numerical method. *Computers & Structures*, **29**, (1994) 1181–1192.

[10] M. Crisfield. *Nonlinear Finite Element Analysis of Solids ans Structures, Vol.2*. John Wiley and Sons, 1st edn. (1997).

[11] J. Batoz and G. Dhatt. *Modélisation des structures par éléments finis*, vol. 1,2,3. Eds Hermès, Paris (1992).

[12] J. Keener and H. Keller. Perturbed bifurcation theory. *Arch. Rational Mech. Anal.*, **50**, (1973) 159–179.

[13] G. Moore and A. Spence. The calculation of turning points of nonlinear equations. *SIAM J. Numer. Anal.*, **17**, (1980) 567–576.

[14] P. Wriggers and J. Simo. A general procedure for the direct calculation of turning and bifurcation points. *Int. J. Numer. Meth. Eng.*, **30**, (1990) 155–176.

[15] A. Eriksson, C. Pacoste and A. Zdunek. Numerical Analysis of complex instability behaviour using incremental-iterative strategies. *Comput. Methods Appl. Mech. Engrg.*, **179**, (1999) 265–305.

[16] E. Boutyour. Détection des bifurcations par des méthodes asymptotiques-numériques. In *Deuxième colloque national en calcul des structures*, vol. 2, 687–692. Giens, France (May 1995).

[17] P. Vannucci, B. Cochelin, N. Damil and M. Potier-Ferry. An asymptotic-numerical method to compute bifurcating branches. *Int. J. Numer. Meth. Eng.*, **41**, (1998) 1365–1389.